Science Advances
AAAS

Supplementary Materials for

Nucleo-cytoplasmic environment modulates spatiotemporal p53 phase separation

Debalina Datta *et al.*

Corresponding author: Samir K. Maji, samirmaji@iitb.ac.in

Sci. Adv. **10**, eads0427 (2024)
DOI: 10.1126/sciadv.ads0427

The PDF file includes:

Other Supplementary Material for this manuscript includes the following:

Supplementary Figures

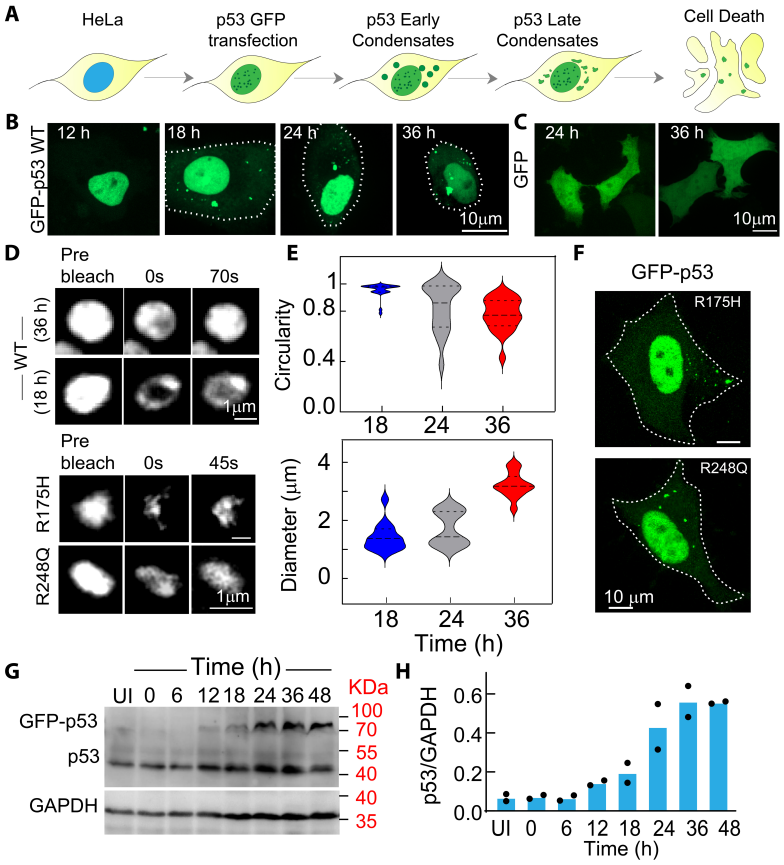

Figure S1. Transient expression of WT and mutant p53 in HeLa cells. (A) Schematic representation of transient transfection, expression of p53-GFP and p53 condensate formation in HeLa cells over time. **(B)** Representative confocal images of HeLa cells over-expressing GFP-p53 over time showing p53 condensate formation. The scale bar is 10 µm. The experiment was performed two independent times. **(C)** HeLa cells expressing only GFP showed pan-cellular diffused localization, where no condensates were observed at 24 h and 36 h. The scale bar is 10 µm. The experiment was performed two independent times. **(D)** Representative confocal images of WT p53 ***(upper panel)*** cytoplasmic condensates during FRAP analysis [pre-bleach, bleach (0 s) and post-bleach (the respective time of recovery in second)] at 18 h and 36 h. FRAP recovery of mutant (R175H and R248Q) ***(lower panel)*** of cytoplasmic condensate at an early time point (18 h). The scale bar is 1 µm. The experiment was performed two independent times. **(E)** Violin plots denoting the quantification of the circularity (***upper panel***) and diameter ***(lower panel)*** of p53 WT cytoplasmic condensates in HeLa cells at 18 h, 24 h and 36 h post-transfection. **(F)** Representative confocal images of HeLa cells expressing GFP p53-R175H and GFP-p53 R248Q at 18 h post-transfection showing p53 mutants condensate formation. The scale bar is 10 µm. The experiment was performed two independent times. **(G)** Western blot showing the expression of GFP-p53 (~71 KDa) and endogenous p53 (~48 KDa) with time in Hela cells post-transfection. UI indicating untransfected control. **(H)** The quantification of Western blot showing the expression of GFP-p53 for n=2 independent experiments.

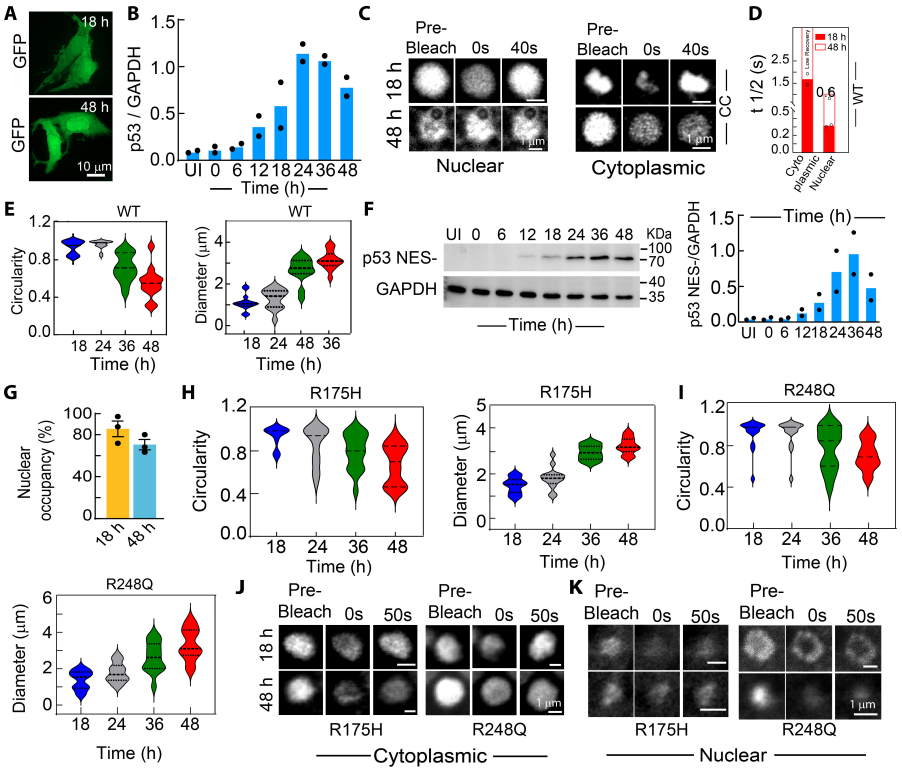

Figure S2. Characterization of WT and mutant p53 in SaOS2 cells. (A) The representative confocal microscopy image of SaOS2 cells expressing only GFP showing pan-cellular diffused localization, where no condensates were observed at 18 h and 48 h. The experiment was performed two independent times. The scale bar is 10 µm. **(B)** Fold change of p53 quantified from the Western blot analysis at indicated time points. **(C)** Representative images of p53 cytoplasmic (CC) and nuclear condensates (NC) during FRAP analysis (pre-bleach, bleach (0 s) and post-bleach (40 s) recovery state of condensates) at 18 h and late 48 h. The scale bar is 1 µm. **(D)** Bar graph representing the $t_{1/2}$ post-bleach of early cytoplasmic and nuclear condensate of p53 in SaOS2 cells. Data represents the mean for n=2 independent experiments. **(E)** Violin plots showing the quantification of the circularity and diameter of WT cytoplasmic p53 condensate showing a decrease in circularity and an increase in the diameter of the condensates over time. **(F)** Western blot showing the expression of NES- p53 with time. UI indicating untransfected control. ***Lower panel:*** Protein levels were quantified from the Western blot analysis at indicated time points. **(G)** ImageJ analysis of nuclear WT GFP-p53 fluorescence showing p53 condensate as the major population at 18 h and 48 h. The quantification was done from the super-resolution microscopy images. **(H-I)** Violin plots measuring the circularity and diameter of cytoplasmic condensates of R175H **(H)** and R248Q **(I)** mutant showing an increase in size and decrease in circularity of condensates with time. (**J, K**) Representative confocal images of the cytoplasmic **(J)** and nuclear **(K)** condensates of R175H and R248Q GFP-p53 during FRAP analysis at 18 and 48 h showing pre-bleach, bleach (0 s) and post-bleach states (50 s). The scale bar is 1 µm. The experiment was performed two independent times.

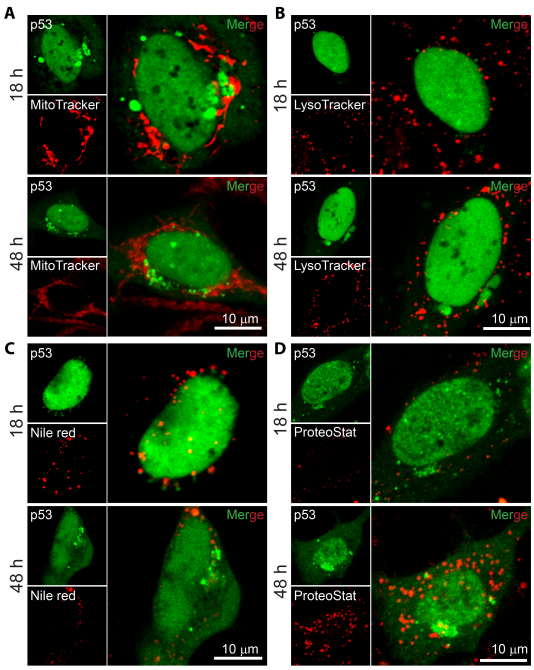

Figure S3. Characterization of cytoplasmic condensates in SaOS2 cells. (A-D) Representative confocal images of MitoTracker **(A)**, LysoTracker **(B)**, Nile Red **(C)** and ProteoStat **(D)** staining at 18 h and 48 h post-transfection of SaOS2 with WT GFP-p53 showing no co-localization with any of the dye/probe. This suggests that the membraneless state of the cytoplasmic condensates is without the association of lysosomes, mitochondria and aggresomes. The scale bar is 10 µm. All the experiments were repeated independently twice with similar results.

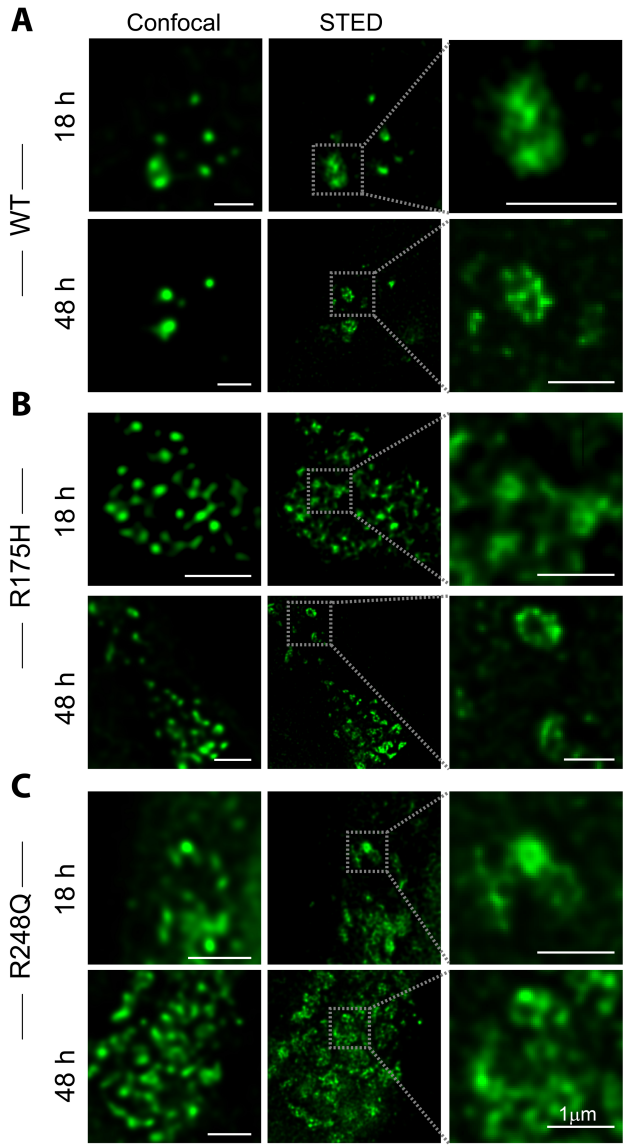

Figure S4. Super-resolution microscopy (STED) of cytoplasmic condensates by WT p53, R175H and R248Q mutant. Super-resolution microscopy images of the cytoplasmic condensates of WT **(A)**, R175H **(B)** and R248Q **(C)** p53 at early (18 h) and late (48 h) time points. The larger cytoplasmic condensates are mostly composed of several small sized condensates. The scale bar is 1 μm. The experiment was repeated twice with similar observations.

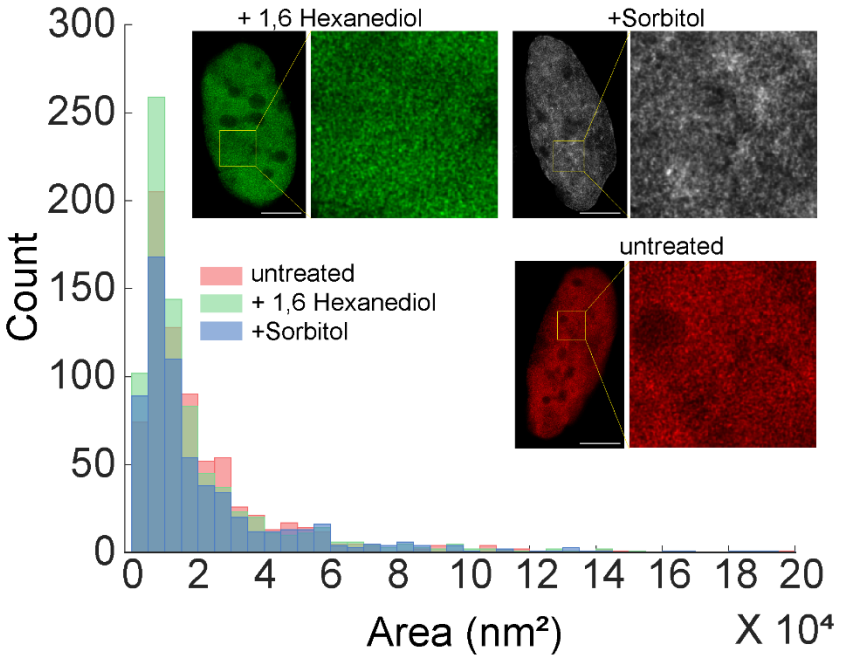

Figure S5. Super-resolution microscopy of nuclear p53 in 1,6 hexanediol and sorbitol treated conditions. Super-resolution STED microscopy images of nuclear p53 in SaOS2 cells expressing GFP-p53 WT, after treatment with 1,6-hexanediol, showed a slightly relative increase of condensates of smaller size, while sorbitol treated cells showed more clustering of nuclear condensates. The scalebar is 5 µm.

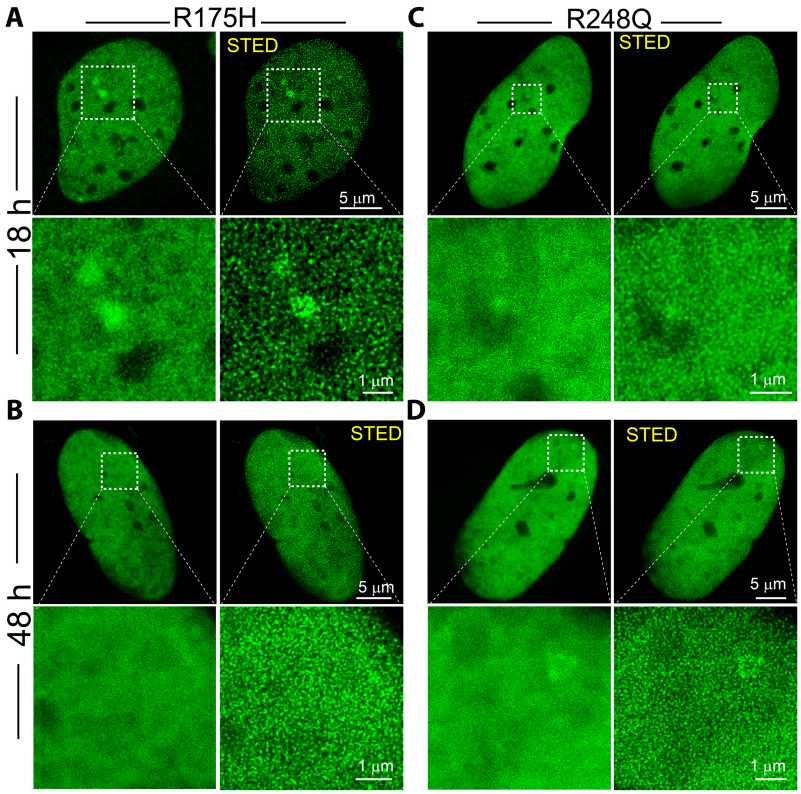

Figure S6. Confocal and super-resolution microscopy of nuclear p53 mutant (R175H and R248Q) condensates in SaOS2 cells. (A, B) Confocal microscopy images showing diffused R175H p53 mutant localization ***(left panel***) in SaOS2 cells at early (18 h) and late (48 h) time points. ***Right panel***: Super-resolution microscopy images using STED showing the R175H p53 condensates throughout the nucleus. **(C, D)** Confocal microscopy images showing diffused R248Q p53 mutant localization ***(left panel)*** in SaOS2 cells at early (18 h) and late (48 h) time points. ***Right panel***: Super-resolution microscopy images using STED showing the R248Q p53 condensates throughout the nucleus. The scale bar is 5 µm**.** The zoomed panels represent the magnified area showing a high density of p53 condensates in the nucleus. The scale bar is 1 µm. All the experiments were performed two independent times.

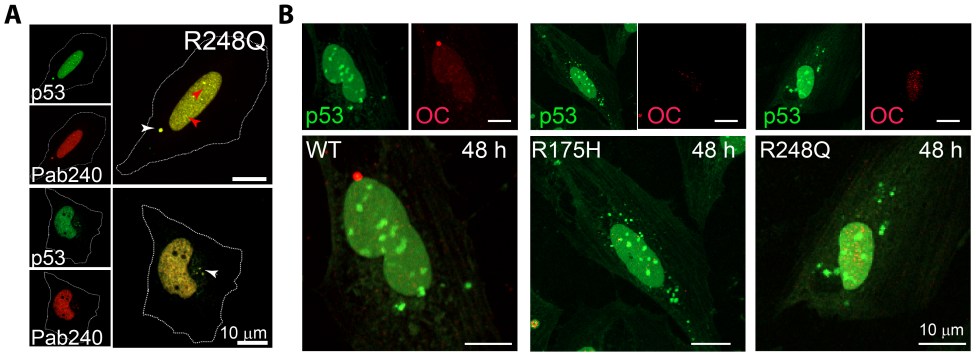

Figure S7. Characterization of WT and mutant p53 in SaOS2 cells. **(A)** Immunofluorescence study showing higher co-localization of R248Q GFP p53 condensates with misfolded p53 specific antibody (Pab240) at 18 h (upper panel) and 48 h (lower panel). The scale bar is 10 µm. (**B**) Immunofluorescence study showing GFP-p53 WT, GFP-p53 R175H and GFP-p53 R248Q condensates did not show any co-localization with OC antibody (specific to amyloid) in the cytoplasm or nucleus. The scale bar is 10 µm. All the experiments were repeated two times independently.

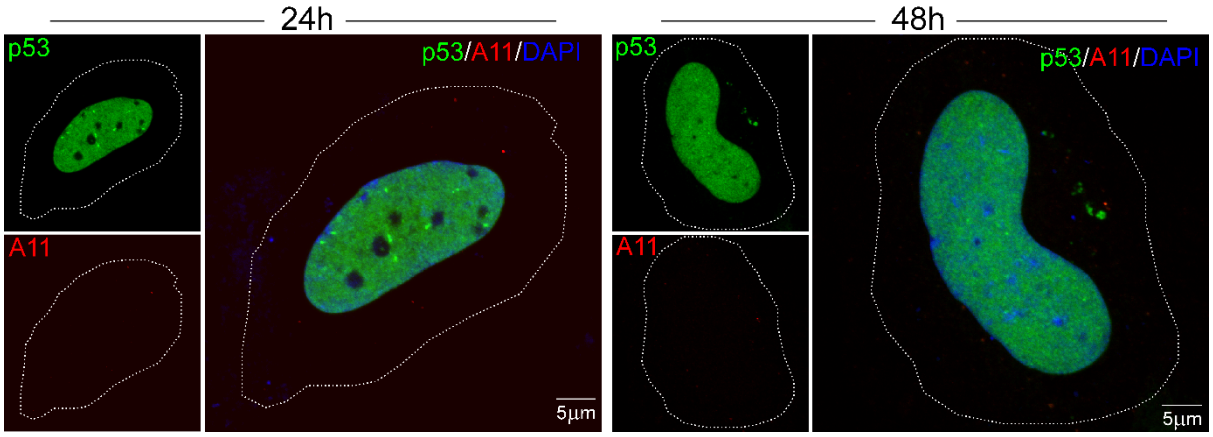

Figure S8. Oligomer characterization of WT p53 in SaOS2 cells. Immunofluorescence study showing no co-localization of nuclear or cytoplasmic p53 with oligomer-specific antibody A11 at 24 h or 48 h time points. The scale bar is 5 µm. All the experiments were repeated two times independently.

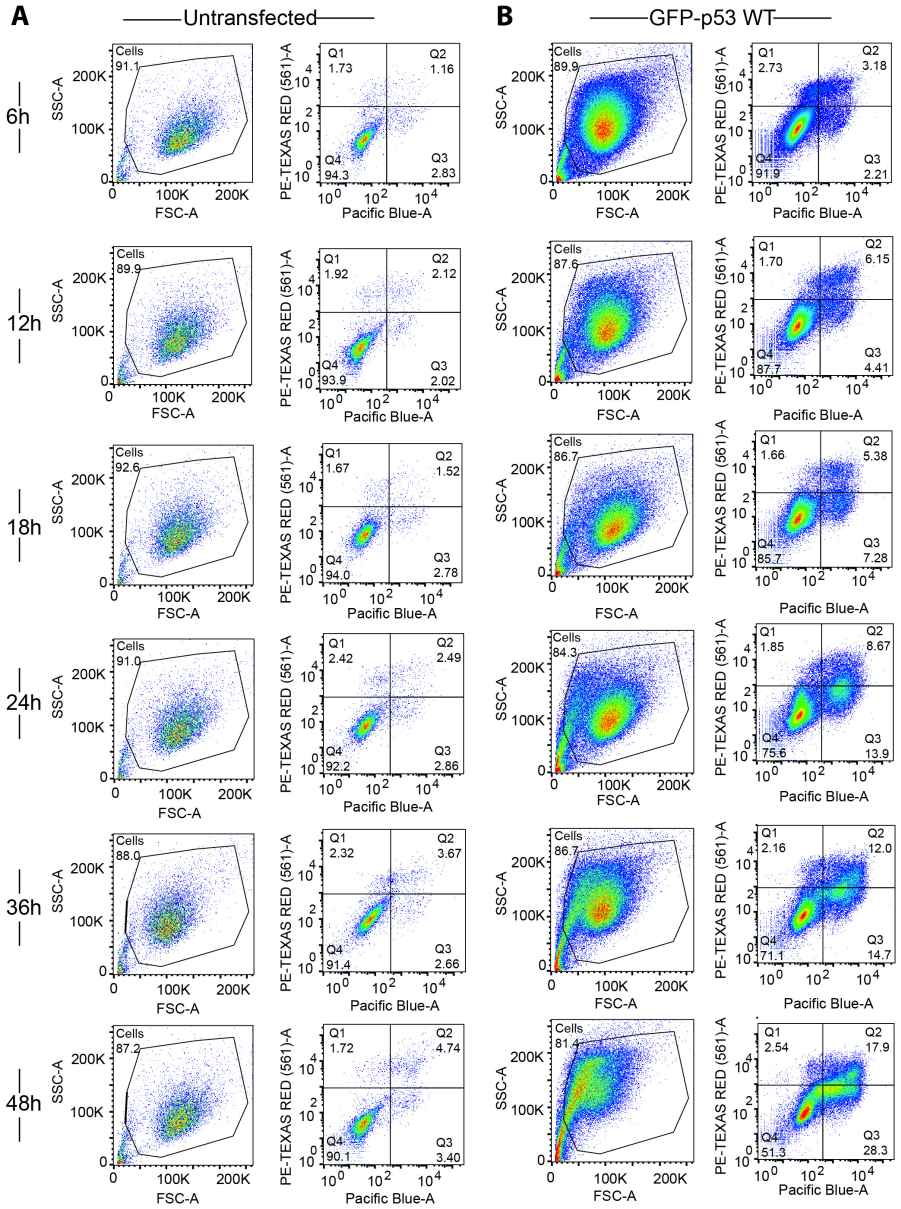

Figure S9. Time-dependent apoptosis assay for SaOS2 cells expressing WT p53. **(A-B)** V450 Annexin V-PI assay followed by FACS analysis showing the apoptotic population of cells transfected with GFP-p53 WT over time. Untransfected cells were used as control and the gating was done with respect to the untransfected cell population. GFP-p53 WT-positive cells (~10^4) were counted to evaluate the apoptotic population. The WT p53 cells showed a lesser apoptotic population at the early time point (6 h, 12 h,18 h), which gradually increased over time (24 h, 36 h, 48 h), indicative of p53 apoptotic function ***(right)***. The values are normalized using untransfected control cells ***(left)***. The experiment was performed two independent times.

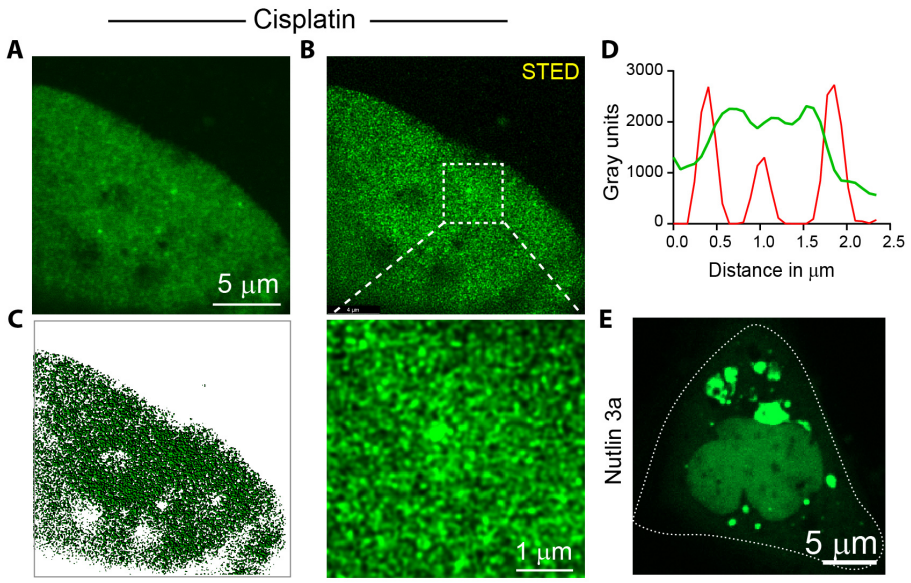

Figure S10. Super-resolution image of nuclear p53 after stabilization and activation. **(A)** Confocal images of GFP-p53 in the nucleus of cells treated with Cisplatin. The scale bar is 5 µm. **(B)** Super-resolution microscopy images using STED showing a dense population of p53 condensates in the nucleus. The magnified image of the nuclear condensates is shown in the lower panel. The scale bar is 1 µm. **(C)** The rendered image of p53 nuclear condensates was obtained from STED microscopy images using IMARIS 8.4. All the experiments were repeated two independent times with similar observations. **(D)** Line profile across the condensate showing no co-localization between p53 condensate and MDM2 **(E)** SaOS2 cells transfected with WT GFP-p53 after treatment with Nutlin showing p53 cytoplasmic condensates at 48 h.

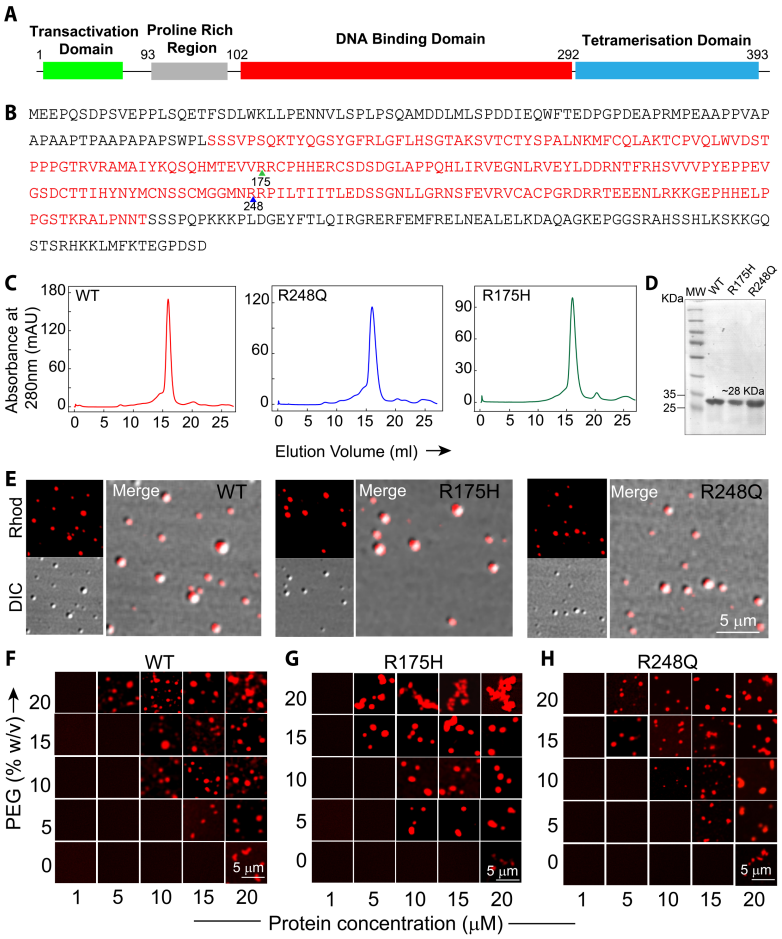

Figure S11. p53C condensate formation *in vitro*. (A) Schematic representation of the domain organization of full-length p53 showing its organization into N-terminal transactivation domain, Proline-rich region, DNA binding domain and tetramerization domain at the C-terminus. **(B)** The primary sequence of full-length p53 comprises 393 amino acids. The DNA binding region (94-312) (p53C) (red) comprises the two mutant sites R175 (green arrow) and R248 (blue arrow), which are two of the hotspot mutations of p53 associated with cancer. **(C)** Size exclusion chromatography profile of purified p53C of WT, R248Q and R175H after expression in BL21 (DE3) cells, purified via Ni-NTA column chromatography. **(D)** 15% SDS-PAGE of all purified p53C proteins showing the single band at ~ 28 kDa, confirming the purity of the protein. **(E)** Representative confocal microscopy images of 10 µM p53C WT (10% v/v labelled to unlabelled protein), and its hotspot mutants R175H and R248Q, showing condensates formation in the presence of 10% (w/v) PEG-8000 in 50 mM sodium phosphate buffer (pH 7.4). The scale bar is 5 µm. The experiment was repeated three times with similar observations. **(F-H)** The phase regime of the NHS-Rhodamine labelled WT, R175H and R248Q p53C (10% v/v labelled to unlabelled protein) showing the LLPS behaviour at different concentrations of protein in the presence of varying percentages of PEG-8000 (0%, 5%, 10%, 15%, and 20% w/v) in 50 mM sodium phosphate buffer (pH 7.4). The data shows a similar protein concentration requirement for condensate formation for both WT and mutant proteins. The scale bar is 5 µm. The experiment was repeated three independent times with similar observations.

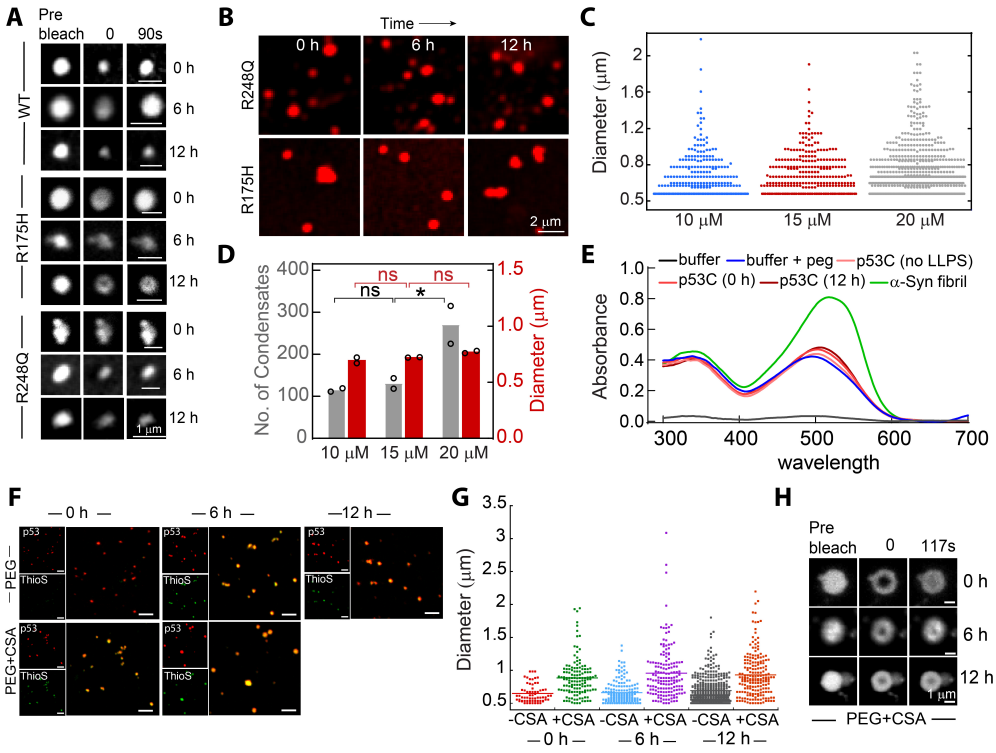

Figure S12. Characterization of WT and mutant p53C. (A) Representative confocal images of WT, R175H and R248Q p53C protein condensates during FRAP analysis (pre-bleach, bleach (0 s), and post-bleach (90 s)] at 0 h, 6 h and 12 h after LLPS. The scale bar is 1 µm. The experiment was performed two independent times. **(B)** Representative confocal images of NHS-Rhodamine labelled (10% v/v labelled to unlabeled protein) of 10 µM R175H and R248Q condensates in the presence of 10% (w/v) PEG-8000 at different time intervals. The scale bar is 2 µm. The experiment was performed three independent times. **(C)** Dot plot representing the size distribution of WT p53C condensates at varying protein concentrations showing a similar size of condensates throughout the concentrations. **(D)** Bar plot representing the number and size of WT p53C condensates at different protein concentrations showing an increase in number but without any significant change in average size (diameter) with an increase in protein concentrations. Statistical significance was calculated with one-way ANOVA using the Student-Newman-Keuls Multiple Comparison post hoc test (*** $p<0.001$, ** $p<0.01$,* $p<0.05$, ns $p>0.05$). **(E)** Congo red (CR) binding assay showing no significant CR binding to WT p53C condensates immediately after formation (0 h) and 12 h after LLPS. p53 without LLPS and α-Syn fibrils were used as control. The experiment was repeated two independent times. **(F)** NHS-Rhodamine labelled (10% v/v labelled to unlabelled protein) WT p53C condensates in the presence of 10% (w/v) PEG-8000 and absence and presence of equimolar concentration of CSA are checked for ThioS partitioning at 0 h, 6 h and 12 h (n=3 independent experiments). Scale bar is 2 µm. **(G)** Dot plot representing the size distribution of WT p53C condensates in the presence and absence of CSA showing larger size of condensates in the presence of CSA at indicated time points. **(H)** Representative confocal images of WT p53C protein condensates in the presence of CSA and 10% PEG-8000 (w/v) during FRAP analysis (pre-bleach, bleach (0 s), and post-bleach (117 s)] at 0 h, 6 h and 12 h after LLPS. The scale bar is 1 µm.

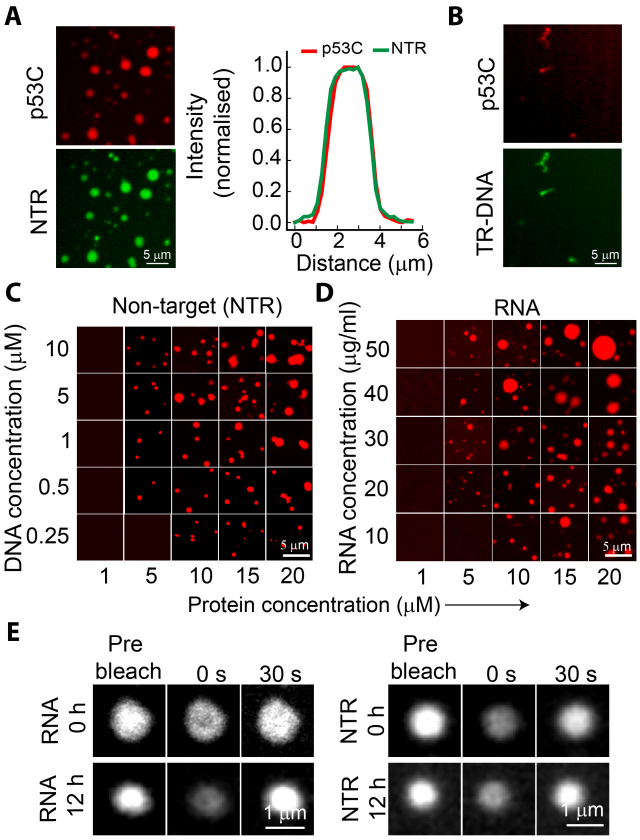

Figure S13. p53C phase separation in the presence of DNA and RNA. **(A)** ***(Left)*** The confocal microscopy images of 20 μM NHS-Rhodamine labelled [10% (v/v) labelled to unlabelled protein] p53C (red) and Atto-488 labelled [10% (v/v) labelled to unlabelled DNA] NTR-DNA (green) corresponding to multicomponent condensate shown in Fig. 5a (inset). ***(Right)*** Line intensity profile showing the co-localization of NHS-Rhodamine labelled p53C with Atto-488 labelled NTR-DNA inside the condensate shown in Fig. 5A (inset). **(B)** The confocal microscopy images showing the remaining small population of foci-like p53 condensates of 20 μM of NHS-Rhodamine labelled [10% (v/v) labelled to unlabelled protein] p53C (red) and Atto-488 labelled [10% (v/v) labelled to unlabelled DNA] TR-DNA (green) corresponding to multicomponent foci shown in Fig. 5a (inset). All the experiments were performed twice with similar observations. **(C, D)** Representative fluorescence microscopy images showing condensate formation by NHS-Rhodamine labelled WT-p53C [10% (v/v) labelled to unlabelled protein] with varying concentrations of NTR-DNA **(C)** and Poly U-RNA **(D)** in the presence of 10% (w/v) PEG-8000 in 50 mM sodium phosphate buffer (pH 7.4). The scale bar is 5 μm. **(E)** Representative confocal images of p53C condensates formed in the presence of RNA and NTR-DNA during FRAP analysis [pre-bleach, bleach (0 s), and post-bleach (30 s)] at 0 h and 12 h after LLPS. The scale bar is 1 μm. The experiment was performed two independent times.

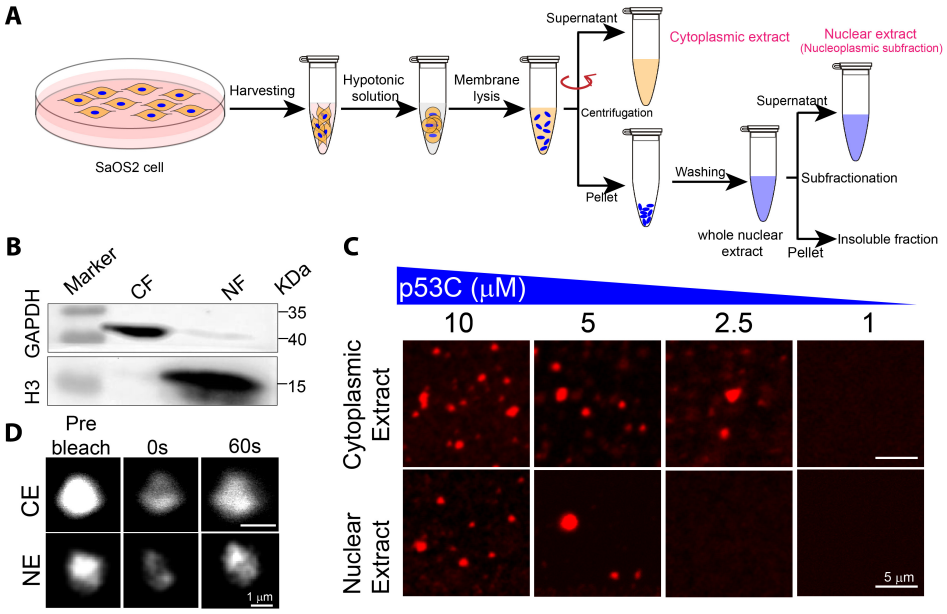

Figure S14. **p53C condensate formation in the presence of nuclear and cytoplasmic extracts of SaOS2. (A)** The schematic representation showing the separation protocol of nuclear and cytoplasmic fractions from SaOS2 cells. **(B)** Western blot of SaOS2 cells extracts showing cytoplasmic marker GAPDH in the cytoplasmic fraction (CF) and nuclear marker H3 in the nuclear fraction (NF) only, indicating the separation of the cytoplasmic and nuclear fractions. **(C)** Representative fluorescence microscopy images of WT p53C [10% (v/v) NHS-Rhodamine labelled to unlabelled protein] condensates at different protein concentrations in the presence of nuclear (NE) and cytoplasmic extract (CE) of SaOS2 cells. The scale bar is 5 μm. The experiment was repeated three times with similar observations. **(D)** Representative images of p53C condensates formed in the cytoplasmic (***upper***) and nuclear (***lower***) extract at pre-bleach, bleach (0 s) and post-bleach states (60 s). The scale bar is 5 μm. The experiment was performed two independent times.

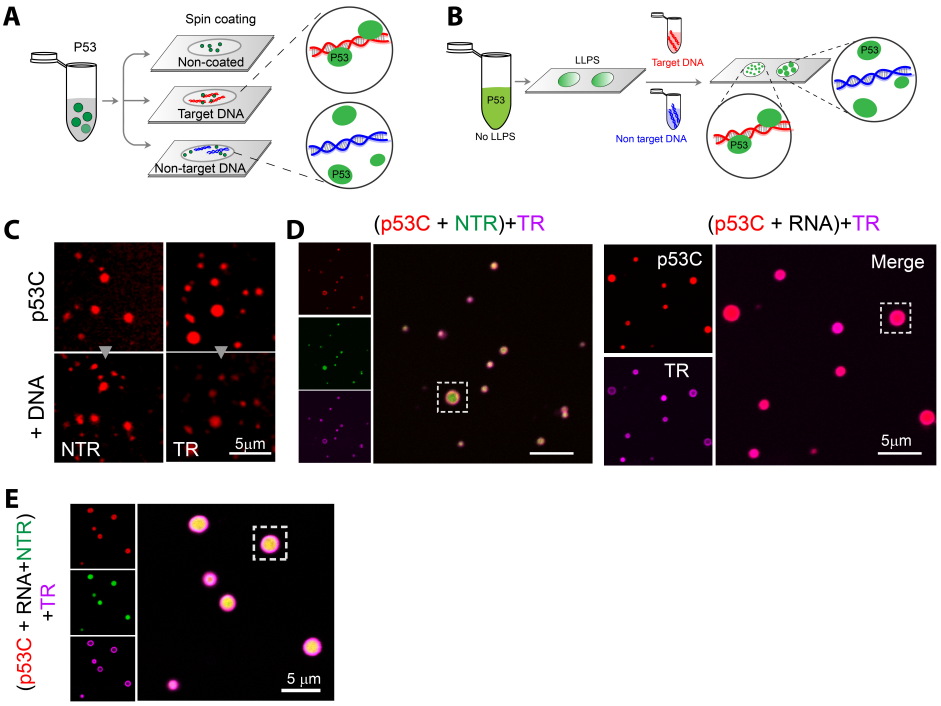

Figure S15. Effect of TR-DNA on pre-formed p53 condensates. (A-B) Schematic representations of the experiments performed to examine the effect of target (TR) and non-target DNA (NTR-DNA) on pre-formed p53C condensates. **(A)** Pre-formed LLPS mixture of p53C formed in the presence of 10% (w/v) PEG-8000 was spotted on glass coverslips that were pre-coated with either TR-DNA or NTR-DNA. **(B)** p53C in the presence of 10% (w/v) PEG-8000 was spotted in chambers on coverslips mounted with silicone isolators (Grace Biolabs). After phase separation, TR-DNA and NTR-DNA were added to the solution in separate chambers and observed under the microscope. **(C)** The confocal microscopy images of p53C condensates in the presence of 10% (w/v) PEG-8000 ***(upper panel)*** showing an increase in the partitioning of p53 into the condensates upon the addition of NTR-DNA, while a decrease in partitioning upon addition of TR-DNA (***lower panel***). The scale bar is 5 µm. The experiment was performed twice with similar results. **(D-E)** Representative confocal microscopy images showing p53C condensates that remained after the addition of Atto 647N labelled TR-DNA to the pre-formed p53C-NTR, p53C-RNA and p53C-NTR-RNA condensates. NTR-DNA was labelled with Atto 488. The inset white box shows condensates represented in the main Figure 6 I-K.

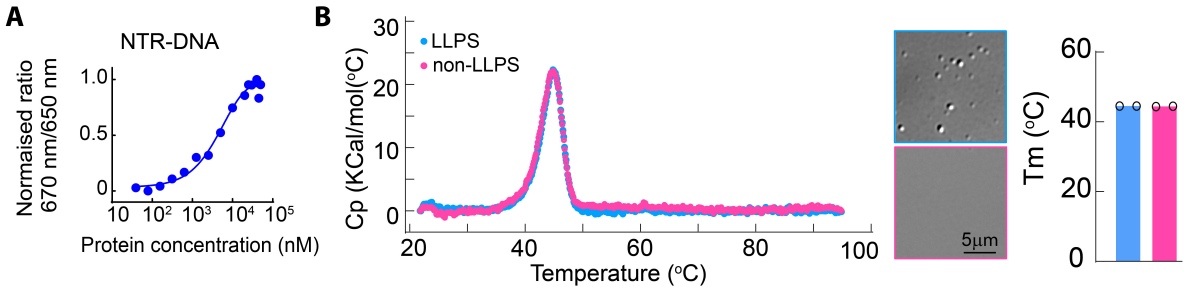

Figure S16. DNA Binding and p53 condensate stability by differential scanning calorimetry (DSC). (A) Spectral shift measurement of p53C (10 µM) in the presence of NTR-DNA showing binding affinity of p53C with nucleic acids. **(B)** The DSC data showing no significant change in melting temperature (T_m). DIC image showing p53C in LLPS and Non-LLPS state (***middle panel***) and corresponding melting T_m (***right panel***).

Table S1. Primers used for site-directed mutagenesis

Name	Sequence Details	Source
R175H- Forward	5'- GGAGGTTGTGAGGCATTGCCCCC - 3'	Sigma
R175H- Reverse	5'- GGGGGCAATGCCTCACAACCTCC - 5'	Sigma
R248Q-Forward	5'- GGGCGGCATGAACCAGAGGCCCATCCTCAC - 3'	Sigma
R248Q-Reverse	5'- GTGAGGATGGGCCTCTGGTTCATGCCGCCC - 3'	Sigma

Table S2. Sequences of Target, Non-Target DNA and RNA used

Nucleic Acid	Sequence details		Source
Target DNA	Forward	5'- ATCAGGAACATGTCCCAACATGTTGAGCTC - 3'	Sigma
	Reverse	5’ - GAGCTCAACATGTTGGGACATGTTCCTGAT - 3’	Sigma
Non-Target DNA	Forward	5’ - AATATGGTTTGAATAAAGAGTAAAGATTTG - 3’	Sigma
	Reverse	5' - CAAATCTTTACTCTTTATTCAAACCATATT - 3'	Sigma
RNA	Poly U RNA		Sigma#9528

Table S3. Primers for qRT-pCR genes (GAPDH and P21)

Gene	**REVERSE (5’-3’)**	**FORWARD (5’-3’)**	**Source**
GAPDH	GGGTTCGAAATGAGGATG	GGGTTCGAAATGAGGATG	Sigma
P21	GGTAGAAATCTGTCATGCTG	AAGACCATGTGGACCTGT	Sigma

SUPPLEMENTARY MOVIE LEGENDS:

Supplementary Movie 1: Time-lapse video of WT GFP-p53 transfected HeLa cells showing cytoplasmic and nuclear condensates exhibiting dynamic nature at 18 h. Time is represented by hh:mm:ss.

Supplementary Movie 2: Time-lapse video showing fusion of cytoplasmic condensates in HeLa cells transfected with WT GFP-p53. Time is represented by hh:mm:ss.

Supplementary Movie 3: Time-lapse video showing fusion of cytoplasmic condensates in SaOS2 cells transfected with WT GFP-p53. Time is represented by hh:mm:ss.

Supplementary Movie 4: Time-lapse video of a single SaOS2 cell, exhibiting spatiotemporal localization of p53, showing the formation of cytoplasmic condensates followed by cell death. Scale bar is 10 μm. Time is represented by hh:mm:ss.

Supplementary Movie 5: Lattice light-sheet microscopy imaging showing the dynamic nature of nuclear condensates in SaOS2 cells transfected with WT GFP-p53 and 18 h and 48 h. Time is represented by mm:ss.

Supplementary Movie 6: Time-lapse video showing the formation of p53C condensates at 20 μM (NHS-Rhodamine labelled p53C 1:10::labelled:unlabelled) *in vitro* with time. Time is represented by mm:ss. Scale bar represents 5 μm.